REFLECTION OF ULTRASONIC WAVES BY AN ARRAY OF MICROCRACKS

Y. C. Angel* and J. D. Achenbach

Department of Civil Engineering
Northwestern University
Evanston, IL 60201

INTRODUCTION

Specular reflection of ultrasonic waves by a flaw plane is affected by the degree of contact of the flaw-plane faces. In general terms, a flaw plane may be viewed as a region where separation zones and contact zones can both exist, and friction may be significant over the contact zones. Achenbach and Norris[1] have proposed a set of nonlinear flaw-plane conditions to account for the separation and friction effects. Other conditions, of a linear type, have been discussed by Thompson and Fiedler[2].

Angel and Achenbach[3,4] have presented an exact analysis of the reflection of elastic waves by a periodic array of cracks. Their results apply to reflection by a flaw plane, under the assumption that the separation zones may be modeled as periodically spaced microcracks which remain stress-free under the action of the incident wave, while the displacements as well as the stresses are continuous over the plane regions between the cracks.

The geometrical configuration analyzed by Angel and Achenbach[3,4] is shown in Fig. 1a. The exact results are, however, rather complicated. The reflected fields are obtained as infinite series of homogeneous and inhomogeneous wave modes. The homogeneous wave modes propagate without decay, while the inhomogeneous modes decay as $|x_2|$ increases. At low frequencies of the incident wave, only the lowest reflected modes are homogeneous, and hence only they have to be taken into account at some distance from the plane of cracks. As the frequency increases, more and more propagating modes are generated, as discussed in some detail elsewhere[4].

Since the exact solution is complicated, we investigate in this paper the applicability of an approximate solution. Thompson and Fiedler[2] have proposed to replace the array of cracks by a layer of

---

*Now at Department of Mechanical Engineering and Materials Science, Rice University, Houston, TX 77001

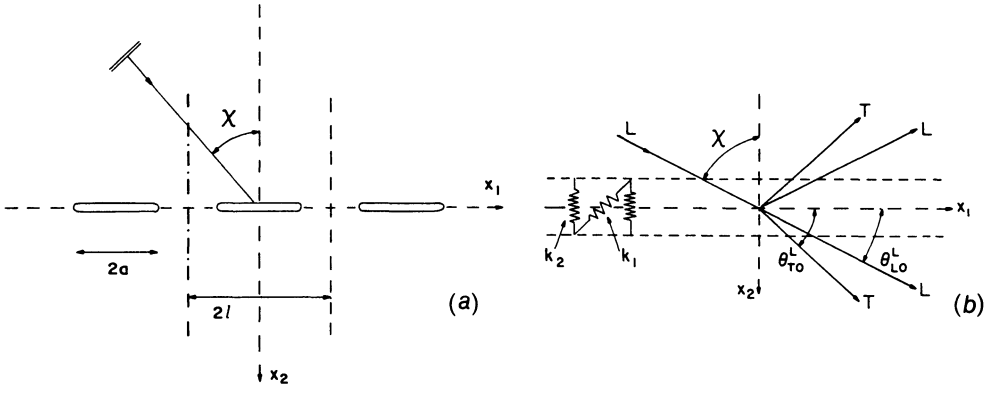

Fig. 1. (a) Plane wave incident on an array of microcracks; (b) Plane wave incident on a layer of massless springs.

massless springs. The geometry for the spring-layer approximation is shown in Fig. 1b. The constant k_2 $\{k_1\}$ of the spring-layer is chosen so that the layer produces the same static displacements as the array of cracks, when the solid is subjected to distant uniform tension {uniform shear}. The method to compute k_1 and k_2, which makes use of results by Tada et al.[5], is discussed in section 9 of Angel and Achenbach[3]. The values of k_1 and k_2 are

$$k_1 = k_2 = -\frac{\pi\mu}{4\ell(1-\nu)} \frac{1}{\log|\cos(\pi a/2\ell)|} \cdot \qquad (1a,b)$$

Here a and ℓ are defined in Fig. 1a, and ν is Poisson's ratio.

In the next Section we consider the incidence of longitudinal and transverse waves on the spring-layer, as shown in Fig. 1b, and we determine the reflection coefficients as functions of the frequency. These results for the spring-layer configuration are compared with exact results for the crack array in the last Section. At low frequencies excellent agreement is observed.

REFLECTION AND TRANSMISSION BY A SPRING LAYER

We consider two half-spaces of identical material properties, which are connected by a layer of massless springs along the plane $x_2 = 0$. The geometry is shown in Fig. 1b.

The displacement vector $\underset{\sim}{U}^{\alpha}(\theta)$ for a plane homogeneous longitudinal wave (α = L) or a plane homogeneous transverse wave (α = T), both of

unit amplitude and propagating in the (x_1,x_2)-plane under an angle θ from the x_1-axis, can be written in the form (no sum on α)

$$\underset{\sim}{U}^{\alpha}(\theta) = \underset{\sim}{d}^{\alpha} \exp(i\omega s_{\alpha} \underset{\sim}{x}\cdot\underset{\sim}{p}), \quad s_L^2 = \rho/(\lambda+2\mu), \quad s_T^2 = \rho/\mu \ , \qquad (2a,b,c)$$

The unit propagation vector $\underset{\sim}{p}$ and the unit displacement vector $\underset{\sim}{d}$, which lie in the (x_1,x_2)-plane, are defined by

$$p_1 = \cos\theta, \quad p_2 = \sin\theta \quad ; \qquad (3)$$

$$\alpha=L: \ d_1^L=\cos\theta, \ d_2^L=\sin\theta; \quad \alpha=T: \ d_1^T= -\sin\theta, \ d_2^T=\cos\theta \ . \qquad (4)$$

The time factor $\exp(-i\omega t)$ is omitted.

The incident wave is defined by (α = L or T)

$$\underset{\sim}{u}_{in}^{L} = u_o \underset{\sim}{U}^{L}(\theta_{Lo}^{L}) \text{ and } \underset{\sim}{u}_{in}^{T} = -u_o \underset{\sim}{U}^{T}(\theta_{To}^{T}), \text{where } \theta_{\alpha o}^{\alpha} = \frac{\pi}{2} - \chi \ . \qquad (5)$$

Reflected and transmitted waves are of the form:

<u>incident longitudinal wave</u>:

reflected longitudinal: $u_o \bar{R}_L^L \underset{\sim}{U}^L(-\theta_{Lo}^L)$; (6a)

reflected transverse: $u_o \bar{R}_T^L \underset{\sim}{U}^T(-\theta_{To}^L)$; (6b)

transmitted longitudinal: $u_o \bar{T}_L^L \underset{\sim}{U}^L(\theta_{Lo}^L)$; (7a)

transmitted transverse: $u_o \bar{T}_T^L \underset{\sim}{U}^T(\theta_{To}^L)$; (7b)

<u>incident transverse wave</u>:

reflected transverse: $u_o \bar{R}_T^T \underset{\sim}{U}^T(-\theta_{To}^T)$; (8a)

reflected longitudinal: $u_o \bar{R}_L^T \underset{\sim}{U}^L(-\theta_{Lo}^T)$; (8b)

transmitted transverse: $u_o \bar{T}_T^T \underset{\sim}{U}^T(\theta_{To}^T)$; (9a)

transmitted longitudinal: $u_o \bar{T}_L^T \underset{\sim}{U}^L(\theta_{Lo}^T)$, (9b)

where $\bar{R}_\beta^\alpha$ and $\bar{T}_\beta^\alpha$ (α,β = L,T) are reflection and transmission coefficients. Here α defines the incident wave and β the reflected or transmitted wave. Across the massless spring-layer the following conditions must be satisfied:

$$\sigma_{22}^{\alpha}(x_1,0^+) = \sigma_{22}^{\alpha}(x_1,0^-); \quad \sigma_{21}^{\alpha}(x_1,0^+) = \sigma_{21}^{\alpha}(x_1,0^-) \ ; \qquad (10a,b)$$

$$\sigma_{22}^{\alpha}(x_1,0^+) = k_2[u_2^{\alpha}(x_1,0^+) - u_2^{\alpha}(x_1,0^-)] \ ;$$

$$\sigma_{21}^{\alpha}(x_1,0^+) = k_1[u_1^{\alpha}(x_1,0^+) - u_1^{\alpha}(x_1,0^-)] \ , \qquad (11a,b)$$

where k_1 and k_2 are the spring constants, as defined by Eq.(1). For an incident longitudinal wave, the relevant stresses at $x_2 = 0^+$ can be compiled from Eq.(7a,b) by using Hooke's law, while the stresses at $x_2 = 0^-$ follow from Eqs.(5) and (6a,b).

A first conclusion of (10)-(11) is the relation

$$\cos\theta_{To}^{L} = \varepsilon \cos\theta_{Lo}^{L} \ , \quad \cos\theta_{Lo}^{T} = \frac{1}{\varepsilon} \cos\theta_{To}^{T} \quad \text{if } \cos\theta_{To}^{T} \leq \varepsilon \qquad (12a,b)$$

where

$$\varepsilon = \frac{c_T}{c_L} = \frac{s_L}{s_T} \ , \quad \text{or} \quad \varepsilon^2 = \frac{1-2\nu}{2(1-\nu)} \ . \qquad (13)$$

Equations (10)-(11) yield a system of four equations for the four complex-valued reflection and transmission coefficients. The system of four equations can be reduced to two systems of two equations by splitting the displacement field into two fields which are symmetric and antisymmetric, respectively, with respect to the plane of the cracks (x_2=0), as illustrated in Fig. 2. Then, the boundary conditions become

$$\sigma_{22}^{\alpha S}(x_1,0^+) = 2k_2 u_2^{\alpha S}(x_1,0^+) \ , \quad \sigma_{21}^{\alpha S}(x_1,0^+) = 0 \ , \qquad (14a,b)$$

$$\sigma_{21}^{\alpha A}(x_1,0^+) = 2k_1 u_1^{\alpha A}(x_1,0^+) \ , \quad \sigma_{22}^{\alpha A}(x_1,0^+) = 0 \ . \qquad (15a,b)$$

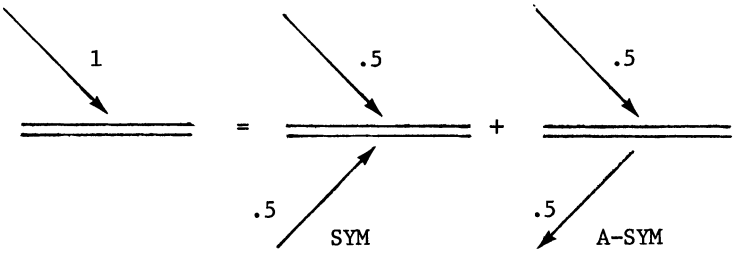

Fig. 2. Decomposition of incident field into symmetric and antisymmetric fields.

The stress corresponding to the displacements of Eqs.(5)-(9) follows directly from Hooke's law. The solution of the four 2 x 2 systems of Eqs.(14)-(15), and subsequent combination of the symmetric and antisymmetric parts, yields the reflected amplitudes of the homogeneous modes in the form

incident longitudinal wave:

$$\bar{R}_L^L = -\bar{\omega}\cos^2(2\theta_{To}^L)(\Delta_2^L)^{-1} + \bar{\omega}\varepsilon^2\sin(2\theta_{Lo}^L)\sin(2\theta_{To}^L)(\Delta_1^L)^{-1}, \quad (16)$$

$$\bar{R}_T^L = -\bar{\omega}\varepsilon\sin(2\theta_{Lo}^L)\cos(2\theta_{To}^L)[(\Delta_2^L)^{-1} + (\Delta_1^L)^{-1}] \quad ; \quad (17)$$

incident transverse wave ($\sin\chi < \varepsilon$) :

$$\bar{R}_T^T = -\bar{\omega}\varepsilon^2\sin(2\theta_{Lo}^T)\sin(2\theta_{To}^T)(\Delta_2^T)^{-1} + \bar{\omega}\cos^2(2\theta_{To}^T)(\Delta_1^T)^{-1}, \quad (18)$$

$$\bar{R}_L^T = -\bar{\omega}\varepsilon\sin(2\theta_{To}^T)\cos(2\theta_{To}^T)[(\Delta_2^T)^{-1} + (\Delta_1^T)^{-1}] \quad ; \quad (19)$$

incident transverse wave ($\sin\chi > \varepsilon$) :

$$\bar{R}_T^T = -2i\bar{\omega}\varepsilon^2\sin(2\theta_{To}^T)p_{Lo}^T[(p_{Lo}^T)^2-1]^{\frac{1}{2}}(\bar{\Delta}_2^T)^{-1} + \bar{\omega}\cos^2(2\theta_{To}^T)(\bar{\Delta}_1^T)^{-1} \quad ; \quad (20)$$

where

$$\bar{\omega} = 2\ell/\lambda_T = \ell\omega/\pi c_T \quad (21)$$

is the dimensionless frequency, and

$$\Delta_2^\alpha = \bar{\omega}D^\alpha + iK_2\sin\theta_{Lo}^\alpha, \quad \Delta_1^\alpha = \bar{\omega}D^\alpha + iK_1\sin\theta_{To}^\alpha, \quad (22a,b)$$

$$K_2 = 2\varepsilon\ell k_2/(\pi\mu), \quad K_1 = 2\ell k_1/(\pi\mu), \quad (23a,b)$$

$$D^\alpha = \cos^2(2\theta_{To}^\alpha) + \varepsilon^2\sin(2\theta_{Lo}^\alpha)\sin(2\theta_{To}^\alpha), \text{ (no sum on } \alpha), \quad (24)$$

$$\bar{\Delta}_2^T = \bar{\omega}\bar{D}^T - K_2[(p_{Lo}^T)^2 - 1]^{\frac{1}{2}}, \quad \bar{\Delta}_1^T = \bar{\omega}\bar{D}^T + iK_1\sin\theta_{To}^T, \quad (25a,b)$$

$$\bar{D}^T = \cos^2(2\theta_{To}^T) + 2i\varepsilon^2\sin(2\theta_{To}^T)p_{Lo}^T[(p_{Lo}^T)^2 - 1]^{\frac{1}{2}} \quad (26)$$

$$p_{Lo}^T = (1/\varepsilon)\sin\chi. \quad (27)$$

The parameters in Eqs.(16)-(20) are: ν, χ, $\bar{a} = a/\ell$ and $\bar{\omega}$.

COMPARISON OF APPROXIMATE AND EXACT REFLECTION COEFFICIENTS

Numerical results are presented in Figs. 3-4. These results were computed for Poisson's ratio $\nu = 0.3$, which yields $\varepsilon \cong 0.535$ and $\arcsin(\varepsilon) \cong 32.3°$, and for $a/\ell = 0.5$. The range of frequencies is such that $0 < \bar{\omega} = 2\ell/\lambda_T < 1$.

Figure 3a shows the exact reflection coefficient R_L^L as computed by Angel and Achenbach[4] - solid line - and $\bar{R}_L^L$ of Eq.(16) - dashed line. Figure 3b shows R_T^L - solid - and $\bar{R}_T^L\Theta^L$ - dashed, where

$$\Theta^L = (\varepsilon\sin\theta_{To}^L/\sin\theta_{Lo}^L)^{\frac{1}{2}}, \quad (28)$$

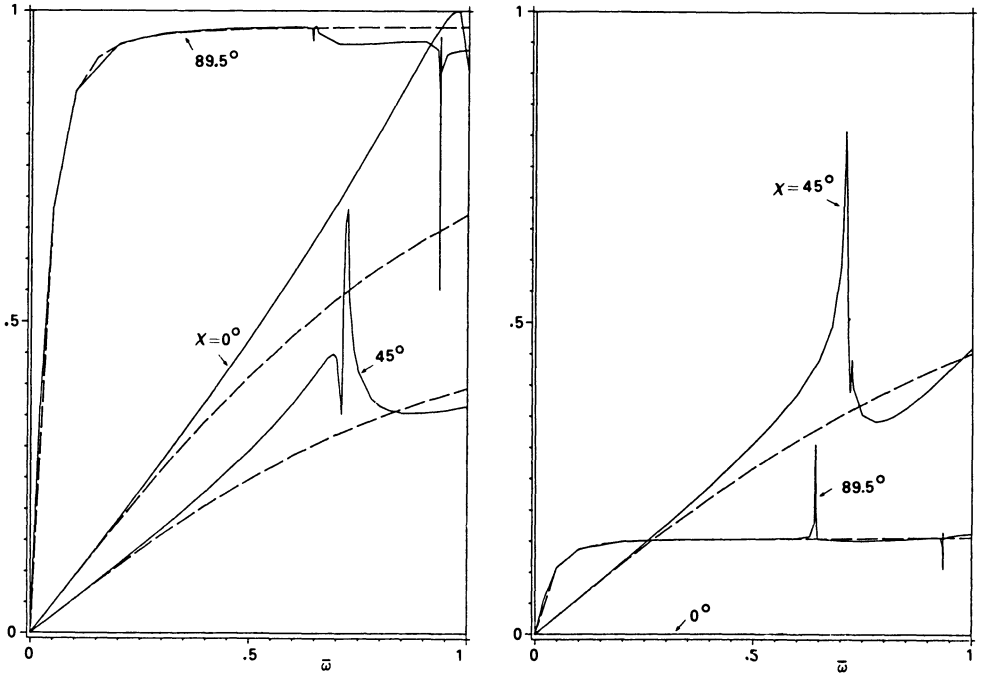

Fig. 3. Moduli of exact coefficients R_β^L (solid lines) and reflection coefficients for spring layer reflection $\bar{R}_\beta^L$ (dashed line) versus $\bar{\omega}$, for an incident longitudinal wave; $a/\ell = 0.5$, $\nu = 0.3$.

and $\bar{R}_T^L$ is defined by Eq.(17). Figure 4 displays the exact reflection coefficient R_T^T - solid - and $\bar{R}_T^T$ of (18) or (20) - dashed. Three angles of incidence have been chosen: $\chi = 0°$, 45°, and 89.5°. For normal incidence ($\chi = 0°$) the coefficients R_T^L and $\bar{R}_T^L$ vanish identically.

In the limit as $\bar{\omega} = 2\ell/\lambda_T = \ell\omega/\pi c_T$ approaches zero, all the coefficients vanish; the cracks appear so small to the incident wave that no reflection occurs. When $\chi = 0°$ or 45°, the dashed curves cannot be distinguished from the solid curves for $\bar{\omega}$ less than 0.2. When $\chi = 89.5°$, the agreement extends to $\bar{\omega} \cong 0.5$, and to $\bar{\omega} = 0.6$ for the curves of Fig. 3b.

As expected, the spring approximation agrees with the exact theory at low frequencies. The approximation does, however, ignore the interference phenomena which occur at increasing frequencies, and which are displayed by the peaks and dips of the solid curves.

ACKNOWLEDGMENT

The work reported here was carried out under Contract DE-AC02-83ERI3036.A002, with the Department of Energy, Office of Basic Energy Sciences, Engineering Research Program.

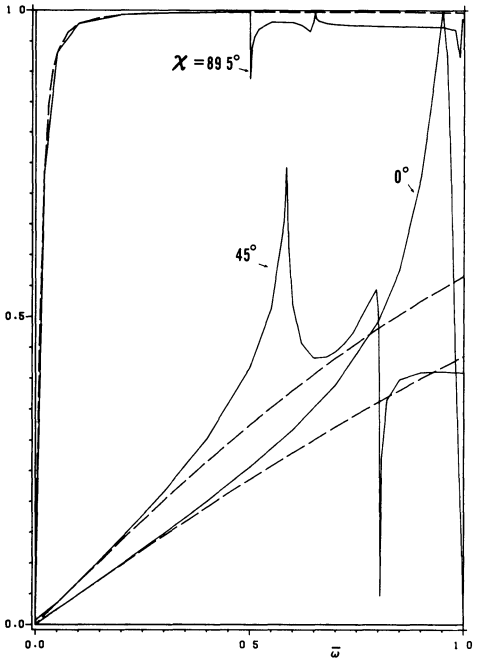

Fig. 4. Moduli of exact coefficients R_T^T (solid lines) and reflection coefficients for spring-layer reflection $\bar{R}_T^T$ (dashed line) versus $\bar{\omega}$ for an incident transverse wave; $a/\ell = 0.5$, $\nu = 0.3$.

REFERENCES

1. J. D. Achenbach and A. N. Norris, Loss of Specular Reflection due to Nonlinear Crack-Face Interaction, J. Nondestructive Evaluation, 3: 229 (1982).
2. R. B. Thompson and C. J. Fiedler, The Effects of Crack Closure on Ultrasonic Scattering Measurements, in "Review of Progress in QNDE 3" D. O. Thompson and D. E. Chimenti,eds, Plenum, New York, p. 207, (1984).
3. Y. C. Angel and J. D. Achenbach, Reflection and Transmission of Elastic Waves by a Periodic Array of Cracks, J. Appl. Mech., to appear.
4. Y. C. Angel and J. D. Achenbach, Reflection and Transmission of Elastic Waves by a Periodic Array of Cracks: Oblique Incidence, submitted for publication.
5. H. Tada, P. Paris, and G. Irwin, The Stress Analysis of Cracks Handbook, Del Research Corporation, St. Louis (1973).